ORIGINAL PAPER

CrossMark

High-Resolution Evaluation of Elastic Properties and Anisotropy of Unconventional Reservoir Rocks via Thermal Core Logging

Evgeny Chekhonin[1] · Evgeny Popov[1] · Yury Popov[1] · Anastasia Gabova[1] · Raisa Romushkevich[1] · Mikhail Spasennykh[1] · Dzhulia Zagranovskaya[2]

Abstract

Unconventional reservoir rocks frequently exhibit considerable degrees of anisotropy, heterogeneity, and high variability of physical rock properties, reflecting the variety of their geological origins. The anisotropy and heterogeneity can have a pronounced impact on sonic log readings, which poses problems since compressional and shear borehole sonic data are traditionally used both as a data source for geomechanical modelling and also for seismic calibration. Sonic logging and acoustic tests in the laboratory use different frequencies due to the small sample sizes in the laboratory, which, along with known complexities in the measurement/interpretation procedure, complicates the characterization of reservoirs in terms of their elastic properties. This paper proposes a new approach to high-resolution evaluation of the elastic properties and anisotropy of unconventional reservoir rocks, based on continuous non-contact, non-destructive high-resolution (0.2–2 mm) thermal profiling of core samples. Variations in measured thermal characteristics (principal thermal conductivity tensor components, volumetric heat capacity, thermal anisotropy coefficient and thermal heterogeneity coefficient) reflect variations in the rock fabric and composition, which also result in the variability of other properties of the rock. More than 100 m of full-diameter cores along three wells drilled in the Bazhenov formation in West Siberia (Russia) have been profiled. The results were combined with sonic well logging data, and correlations between components of thermal conductivity, density and acoustic velocities were established, as well as correlations between thermal anisotropy, Young's modulus anisotropy and Thomsen's parameters. Examples of high-resolution prediction of velocities, density, elastic modulus, and anisotropy parameters based on the results of thermal core logging are given, together with the respective verification.

Keywords Anisotropy · Elastic properties · Thermal properties · Unconventional rocks · Thermal core logging · Optical scanning

1 Introduction

Many of the tasks that are addressed in rock mechanics and rock engineering depend on reliable measurements of the elastic properties and anisotropy of rocks, and on the interpretation and incorporation of those measurement results into geomechanical models. In petroleum geomechanics these parameters are usually estimated from sonic logging and a restricted number of laboratory measurements.

However, the use of traditional measurement techniques is sometimes impossible due to low quality of the acoustic logging signal or of core samples. Spatial resolution of sonic logging data is limited by the distance between receivers and the number of receivers processed simultaneously during interpretation. Shale anisotropy due to strong layering can have a pronounced impact on sonic log readings, which are critical for various disciplines (Keir et al. 2011). Estimation of the strength of anisotropy in a transverse isotropy medium with a vertical axis of symmetry (TIV medium) requires specific analysis when logging is carried out in vertical wells (Suarez-Rivera and Bratton 2009). Studies in a laboratory are non-continuous, time-consuming (particularly as regards core selection and preparation) and often unreliable due to geomechanical test features, rock heterogeneity, and rock anisotropy. When studying anisotropic rocks in the lab, rock

✉ Evgeny Chekhonin
   E.Chekhonin@skoltech.ru

1   Skolkovo Institute of Science and Technology, 3 Nobel Street, Moscow 121205, Russia

2   LLC Gazpromneft Scientific and Technical Center, 75-79D Moika river emb., St. Petersburg 190000, Russia

specimens must be drilled in different directions (Armstrong et al. 1994), and heterogeneity of the full-diameter core sample (from which specimens are sampled in different orientations) is a major impediment to reliable evaluation of the anisotropy. In addition, this approach leads to destruction of the core sample under study. There is a method for characterizing the deformation anisotropy of rock from a single triaxial test on a single specimen (Togashi et al. 2017). But it requires special preparation of the specimen (often not possible due to the state of the core), modification of the measuring cup and comprehensive metrological testing.

The development and application of an optical scanning technique for rock thermal property measurements (thermal conductivity, thermal diffusivity, and volumetric heat capacity) (Chekhonin et al. 2012) creates exciting new possibilities in rock mechanics and rock engineering (Popov et al. 2016a). The technique allows to record detailed profiles of the rock thermal properties and to estimate thermal heterogeneity and anisotropy of rocks reflect variations in the rock fabric and composition that also drive the variability of other rock properties. A few papers have been written on correlations between sonic wave velocities and thermal conductivities (they include Popov et al. 2003; Özkahraman et al. 2004; Kim et al. 2012; Pimienta et al. 2014), but no one has before dealt with continuous high-quality distributions of the thermal properties when extended sonic logging data are also available. This is explained mainly by the lack or insufficient amount of reliable experimental data on thermal properties due to the shortcomings of conventional approaches to the measurement of such properties (Popov et al. 2016b).

There is no published coupled analysis (based on real data) of both components of thermal conductivity (along and across rock bedding), compressional and shear wave velocities, density, thermal anisotropy coefficient, Young's modulus anisotropy and Thomsen's parameters. Our first attempt (Popov et al. 2015) at combining sonic logging and continuous thermal conductivity measurements on core samples from a well in West Siberia showed that both thermal anisotropy and shear wave anisotropy are related to rock texture and are well correlated in an unconventional formation (TIV medium). Results of thermal anisotropy analysis were used to evaluate elastic anisotropy in intervals where the well conditions did not allow rock anisotropy to be estimated from the sonic logging data. New data, obtained from several wells at another oilfield (Chekhonin et al. 2016), established a strong correlation between components of thermal conductivity tensor and elastic wave velocities in the Bazhenov formation. It was demonstrated that elastic moduli and Young's modulus anisotropy could be predicted via the data on rock thermal conductivity and thermal anisotropy.

2 Object of the Research and Geological Setting

More than 100 m or 1062 full-diameter core samples were continuously analyzed along with logging data from three wells drilled through the Bazhenov formation at an oilfield in the West Siberian Basin, which is the largest petroleum basin in the world (Ulmishek 2003). The studied Bazhenov deposits are composed of clayous, siliceous, and carbonate minerals in various proportions. The rocks contain pyrite in a thin-scattered form, in the form of framboids and laminas. The rocks have a pelitic structure, with thin flaggy, foliate, and lamellate texture. They were deposited in a marine environment and are composed primarily of siliceous minerals (Fig. 1), rich in planctonic type II organic matter.

Kerogen accumulations have elliptical, spotted, and sparry forms and are distributed in the rock matrix either uniformly, or in the form of spots and layered-plane horizontal-lenticular fibers. Kerogen content in the rocks under study varies from 2.5 to 20 wt% (6.5 wt% in average). Micropores (2–6 microns) in the rocks are uniformly distributed for the most part and create a cellular microporous structure of laminas. Open porosity (measured with helium) varies from 0.33 to 6.95% (average porosity is 1.10%) and
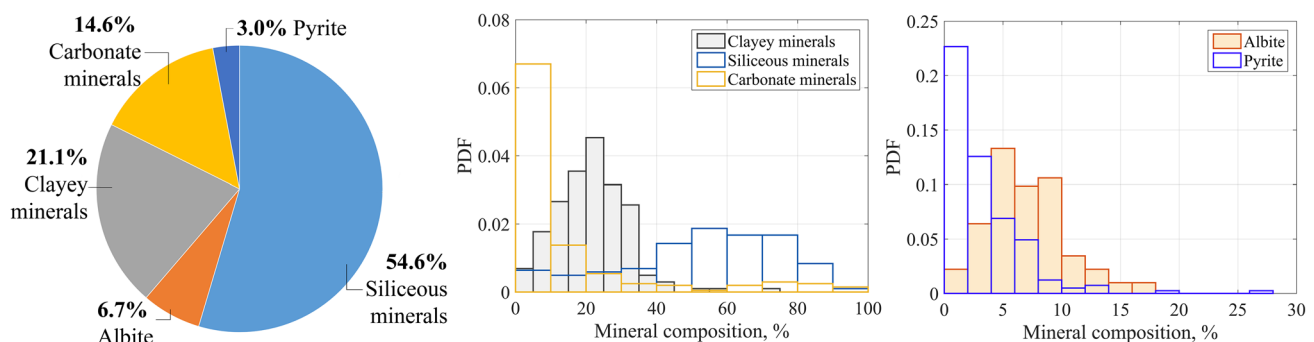

Fig. 1 Mineral composition of the Bazhenov formation rocks and corresponding histograms of each mineral component from three wells drilled at the same oilfield in the West Siberian Basin. 'PDF' represents an estimate of probability density function

the rock permeability range is from 0.001 to 0.975 mD with average value of 0.064 mD. For purposes of the discussion below it should be mentioned that, as shown by core and log data analysis, the Bazhenov formation at the studied wells has TI anisotropy with a vertical axis of symmetry.

3 Investigation Methods and Field Data

3.1 Thermal Core Logging

The thermal core logging technique is based on the optical scanning (OS) instrument application (Fig. 2a) [the instrument is being manufactured by "Lippmann & Rauen GbR" company (http://www.tcscan.de)], where the flat or cylindrical surface of a rock sample is heated by a focused, mobile and continuously operated optical heat source mounted with an array of three infrared temperature sensors in a so-called "optical head". The optical head is moved at a constant velocity relative to the rock sample (Popov et al. 2016a). Thermal properties of the sample are determined by solution of the thermal diffusivity equation for a quasi-stationary temperature field in a movable coordinate system (with the origin in the heat spot center on the surface of the sample). The instrument used in the study is a new modification to an earlier version (described in Popov 1997). It provides continuous non-contact measurement of thermal conductivity and volumetric heat capacity on full-diameter cores, core samples, core plugs, broken cores, and other types of rock samples. Continuous profiles enable measurement of the heterogeneity and structural–textural features of rocks with spatial resolution of 0.2–1 mm. Principal axes of thermal anisotropy can be established from several non-parallel optical scannings. If the rock bedding plane is perpendicular to a flat surface of the rock sample and rock anisotropy can be described with a 2D anisotropy model, the thermal conductivity tensor components of the rock can be determined from two optical scannings: along and perpendicular to the bedding plane (Fig. 2b). Essential features of the optical scanning measurements, of the instrument used and of our approaches to rock anisotropy and heterogeneity are described in detail in Popov et al. (2016a). The method is universally recognized and tested, and is included in ISRM suggested methods for determining the thermal properties of rocks (Popov et al. 2016b).

Thermal anisotropy is calculated for each scanned core sample as $K_T = \lambda_\| / \lambda_\perp$, where $\lambda_\|$ is the parallel to bedding component of thermal conductivity and $\lambda_\perp$ is the perpendicular to bedding thermal conductivity component for every core sample.

3.2 Borehole Acoustic and Density Logging

Acoustic logging was performed with a sonic scanner tool (Franco et al. 2006), openhole at all wells. Estimation of interval transit times (slownesses) was carried out with far-monopole and cross-dipole transmitter data using a standard technique based on analysis of the coherence

Fig. 2 Optical scanning instrument (**a**) for thermal core logging and determination of the principal thermal conductivity tensor components of VTI shales (**b**) from two scannings: along (line 2) and perpendicular (line 1) to the bedding plane. If scanning is performed at an angle to the bedding plane, the principal components of the thermal conductivity tensor can be calculated using formulas from Popov and Mandel (1998)
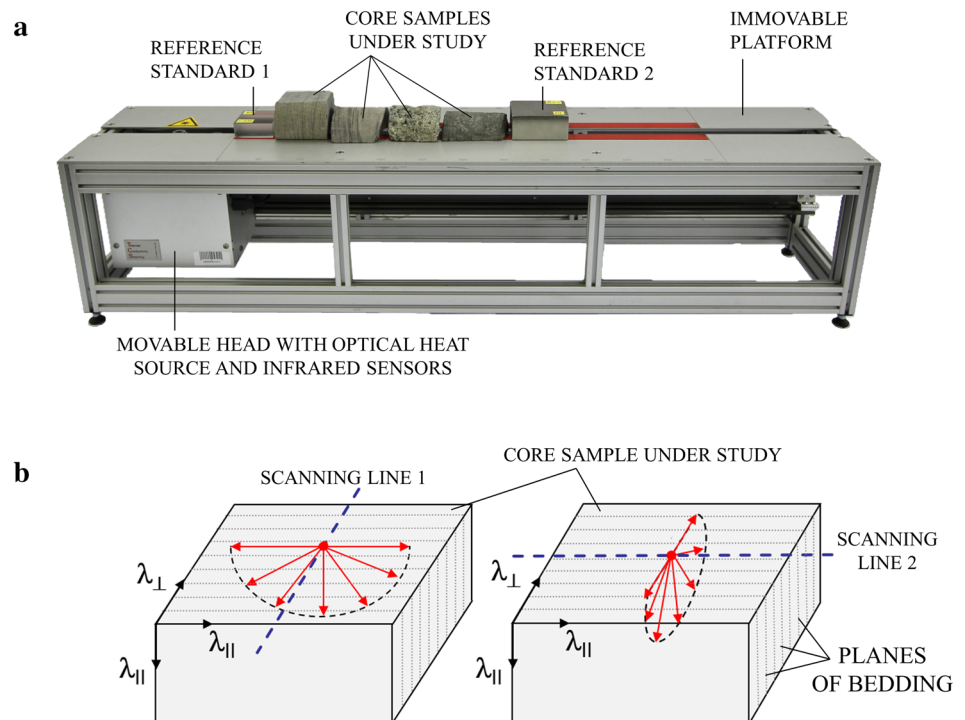
of wave packets in a transmitter–receiver system (Pistre and Sinha 2008). The Alford Rotation technique (Alford 1986) was used to transform cross-dipole data into a fast- and slow shear dipole data set. The slowness estimation was carried out using five receivers with total vertical resolution of 0.6 m, and slowness anisotropy (the relative difference between fast and slow shear slownesses) with vertical resolution about 1 m corresponding to the length of the receiver array (Brie et al. 1998). The shear wave polarized in a horizontal direction was estimated by a multistep procedure based on inversion of the Stoneley wave dispersion curve over the entire frequency range using the STRVP (Stoneley radial velocity profiling) data processing algorithm (Pistre and Sinha 2008).

The bulk formation density was measured using Platform Express integrated wireline logging tool with 'standard' vertical resolution of 20.3 cm (Goligher et al. 1996).

The quality of the considered well logs in the Bazhenov section of the wells was estimated by experts as good.

4 Experimental Results and Analysis

4.1 Thermal Properties, Elastic Waves and Density

Profiles of principal thermal conductivity tensor components and thermal anisotropy coefficient were processed in sequence for every core sample from the Bazhenov formation (see Fig. 2b) and stacked. The results are shown in Fig. 3 along with corresponding histograms, where the number of bins was chosen according to Scott's rule (Scott 1979). Distribution of thermal conductivity components and thermal anisotropy are unimodal and right-skewed (positive-skew) due to the presence of (1) small-size (< 1 cm) pyrite inclusions in the form of framboids and laminas, (2) primarily of siliceous rocks (with SiO_2 content of more than 70%). The different numbers "n" of elements on the plots in Fig. 3 are explained by high thermal heterogeneity of some core samples and by the fact that it was sometimes impossible to measure both principal components of thermal conductivity tensor due to inappropriate state of the core sample. Several core samples with thermal conductivity higher than 3.5 W/(m·K) are excluded from further analysis due to the presence
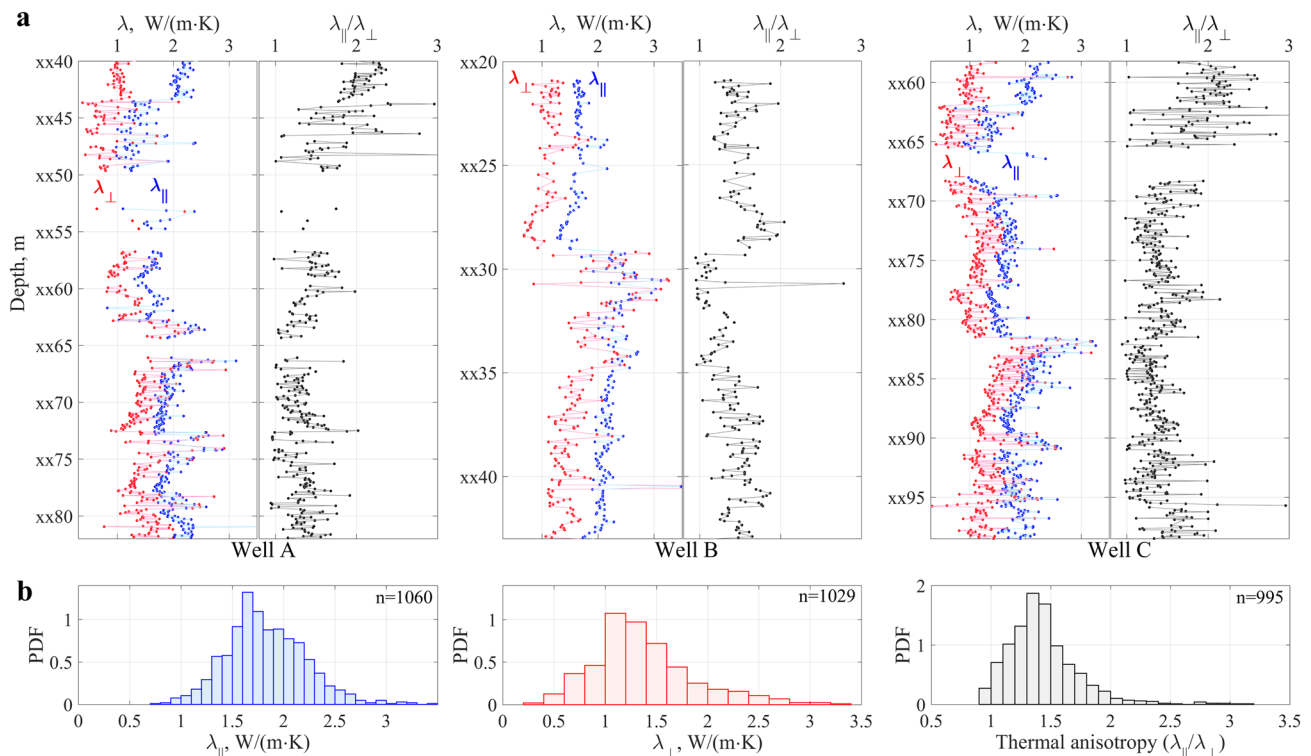

Fig. 3 Profiles along wells (**a**) and general histograms (**b**) of principal thermal conductivity tensor components (perpendicular to bedding in red, parallel to bedding in blue) and thermal anisotropy coefficient on the core scale (~ 10 cm on average). Every point on the plot **a** represents average thermal conductivity or thermal anisotropy coef-ficient value of a core sample. 'PDF' represents an estimate of probability density function (the area of each bar is the relative number of observations, the sum of the bar areas is 1). The first two digits for the depths are hidden because of confidentiality

of pyrite inclusions of about 1 cm: thermal conductivity of pyrite minerals is 41.4 W/(m·K) while thermal conductivity of any other constituent elements of the Bazhenov formation does not exceed 3.2 W/(m·K) (Popov et al. 1987). The experimental data in Fig. 3 show major variations (up to several times) of thermal conductivity and thermal anisotropy coefficient along the wells within depth intervals of the Bazhenov formation on a core scale up to dozens of meters.

Compressive wave velocity V_P, shear wave velocity V_S, and density ρ variations with depth are presented below (Sect. 5, black curves in Figs. 7, 8) in the discussion of how wave velocity and density forecasts are obtained from the results of thermal conductivity profiling.

To find correlations between elastic wave velocities and thermal conductivity, results of thermal core profiling were initially upscaled (using a "window" with length of 60 cm) to the value of the vertical resolution of the sonic logging tool. A strong correlation between both components of thermal conductivity and acoustic velocities was established (Fig. 4a). Rare data outside 99% prediction interval was excluded during the analysis. Thermal conductivity components were initially upscaled to the scale of density data to analyze the corresponding correlation with density (Fig. 4b). The small cloud of points outside the 99% prediction interval in Fig. 4b corresponds to several depth intervals where

density measured in lab is systematically less than logging density (this can be explained by enhanced core unloading after core recovery from a well to the surface). The results in Fig. 4 show that the closest correlation of both velocities and density with thermal conductivity is observed with the component $\lambda_{\parallel}$ of thermal conductivity, which mainly reflects changes in organic content and mineralogy. For the oilfield being investigated, use of a multiple regression $V_P(\lambda_{\parallel}, \lambda_{\perp})$ or $V_S(\lambda_{\parallel}, \lambda_{\perp})$ did not improve the coefficient of determination R^2 in comparison with one thermal conductivity component, while use of a multiple regression for bulk density $\rho(\lambda_{\parallel}, \lambda_{\perp})$ improved R^2 significantly:

$$\rho(\lambda_{\parallel}, \lambda_{\perp}) = 1.905 + 0.318\lambda_{\parallel} - 0.144\lambda_{\perp} \quad (R^2 = 0.539, \sigma = 0.055).$$
(1)

Here and elsewhere, the symbol σ means root mean squared error (standard error).

Established correlations are used for V_P, V_S and ρ prognosis via thermal core logging (Sect. 5.1 below).

4.2 Thermal and Elastic Anisotropy

Shear wave slowness anisotropy (calculated by dividing the difference between fast and slow shear slownesses by their average) is about 1% on average and does not exceed 5%
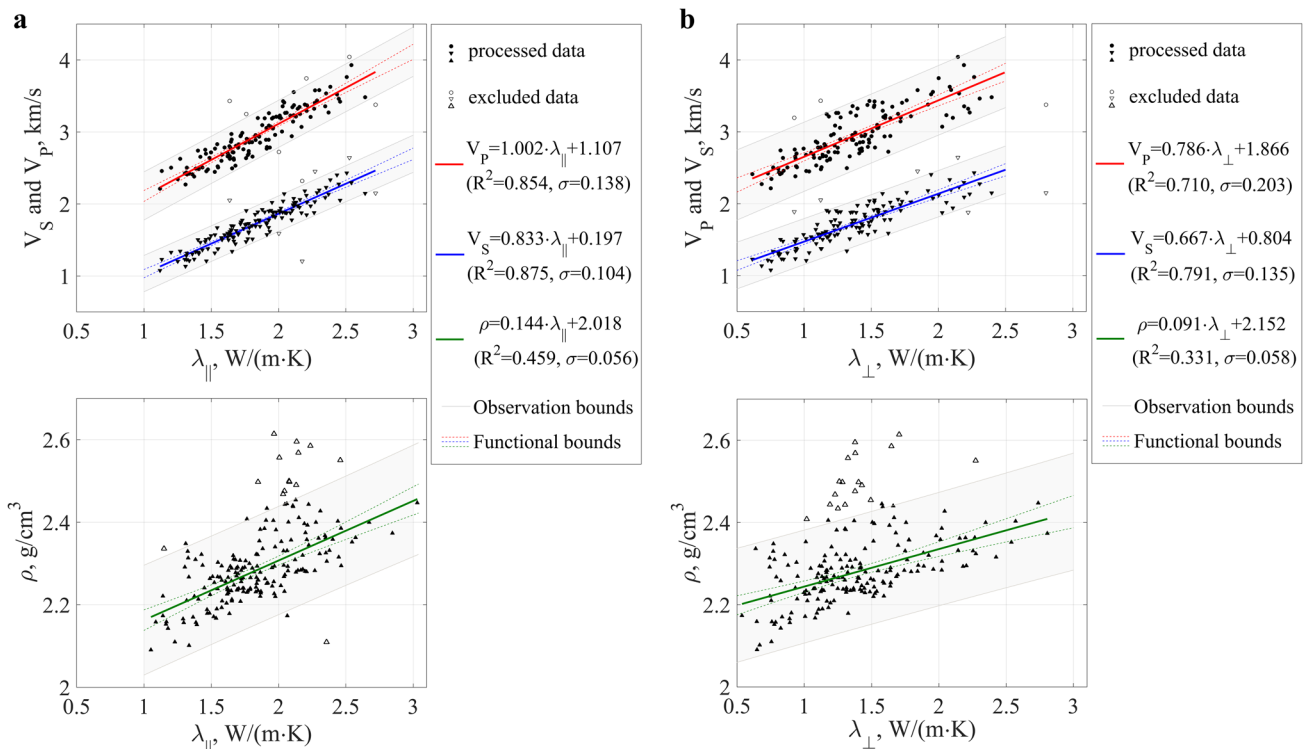

Fig. 4 Scatter plots of elastic wave velocities (V_P, V_S) and bulk density (ρ) versus parallel (**a**) and perpendicular (**b**) components of thermal conductivity. Linear regression lines (red for V_P, blue for V_S, and green for ρ) are shown with upper and lower 99% prediction bounds for a new observation (grey lines) or for the fitted curve (dashed colored lines)

in some short intervals of studied vertical wells. Together with findings from the analysis of minimum and maximum offline energies (Franco et al. 2006), this implies that the studied intervals exhibit negligible azimuthal anisotropy. At the same time, the Bazhenov formation in the given region is characterized by significant variations of thermal anisotropy coefficient (up to 3) (Fig. 3), negligible azimuthal thermal anisotropy (measured on flat ends of a core sample), and can, therefore, be considered to be a transversely isotropic medium with a vertical axis of symmetry.

According to (Thomsen 1986), anisotropy in a TIV medium can be described by three anisotropy parameters, ε, δ, and γ. The γ parameter for the three wells under consideration was calculated using V_{SV} (registered directly, denoted as V_S in this text) and V_{SH} (estimated using the multifrequent inversion of a Stoneley wave) according to (Tsvankin 2012)

$$\gamma = \frac{C_{66} - C_{44}}{2C_{44}} = \frac{V_{SH}^2 - V_{SV}^2}{2V_{SV}^2}, \tag{2}$$

and can be considered to be shear wave anisotropy. The ε parameter was calculated according to (Tsvankin 2012) using measured V_{PV} (denoted as V_P in this text) and V_{PH} estimated via a modified ANNIE approximation (Suarez-Rivera and Bratton 2009)

$$\varepsilon = \frac{C_{11} - C_{33}}{2C_{33}} = \frac{V_{PH}^2 - V_{PV}^2}{2V_{PV}^2}, \tag{3}$$

and can be considered to be a compressional wave anisotropy. C_{ij} are stiffness coefficients, V_{PH} and V_{SH} are the P-wave and S-wave velocities parallel to the bedding plane, V_{PV} and V_{SV} are P-wave and S-wave velocities normal to the bedding plane. Modified ANNIE approximation involves two characterization parameters in ANNIE approximation of

Schoenberg et al. (1996), which is based on the assumption of two relationships ($C_{12} = C_{13} = C_{33} - 2C_{44}$) and generally used in the seismic community to represent the behavior of laminated media (e.g., shale).

Scatter plots of elastic anisotropy parameters and thermal anisotropy coefficient (calculated as the ratio of thermal conductivity parallel to the bedding plane to thermal conductivity normal to the bedding plane and initially upscaled to the vertical resolution of sonic logging data) are shown in Fig. 5. The correlations are quite close, especially if multiple correlation is used (including the parallel component of thermal conductivity in addition to thermal anisotropy coefficient).

Figure 5 includes negative values of Thomsen's γ and ε parameters. These values are located at several depth intervals where there are vertical cracks of technogenic origin (e.g., caused by work on the well). These cracks are clearly visible on the resistivity images from the Fullbore Formation MicroImager (FMI) (Brown et al. 2015). An example of dynamic images (i.e., in case when image normalization is done dynamically by considering formation resistivity ranges in a sliding window to amplify resistivity contrasts, see details in Brown et al. 2015) is shown in Fig. 6.

Anisotropy of Young's modulus was calculated as the ratio of Young's modulus E_H parallel to bedding to Young's modulus E_V perpendicular to bedding

$$K_E = \frac{E_H}{E_V} = \frac{C_{11}C_{22} - C_{12}^2}{C_{22}C_{33} - C_{23}^2}, \tag{4}$$

where $C_{22} = C_{11}$, $C_{12} = C_{11} - 2C_{66}$ due to the symmetry and C_{23} was estimated using a modified ANNIE approximation (Suarez-Rivera and Bratton 2009). A cross-plot of Young's modulus anisotropy versus thermal anisotropy is shown in Fig. 7. The correlations are quite close, especially if multiple correlation is used.
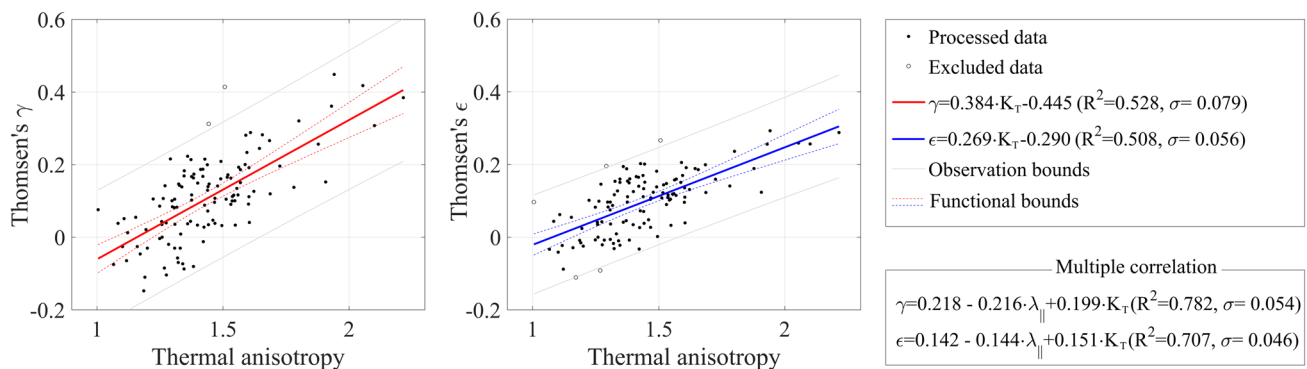

Fig. 5 Scatter plots of Thomsen's parameters versus thermal anisotropy coefficient K_T. Linear regression lines (colored lines) are shown with upper and lower 99% prediction bounds for a new observation (grey lines) or for the fitted curve (dashed lines in colors). The fit can be improved by taking into account the parallel component of thermal conductivity, as seen from the multiple correlation box

Fig. 6 Parts of an FMI resistivity images from three wells showing the presence of vertical cracks of technogenic origin (colored in red); green lines denote layer boundaries. Microresistivity data are processed and assigned a color scale: conductive features are represented by dark colors and resistive features are represented by light colors
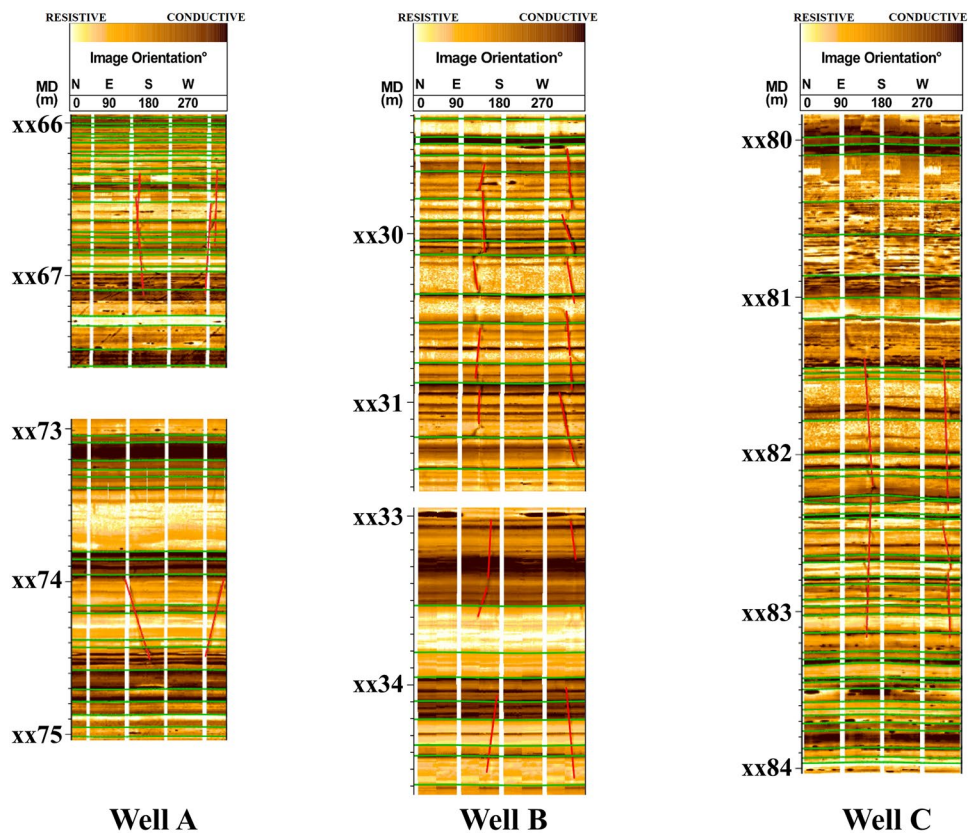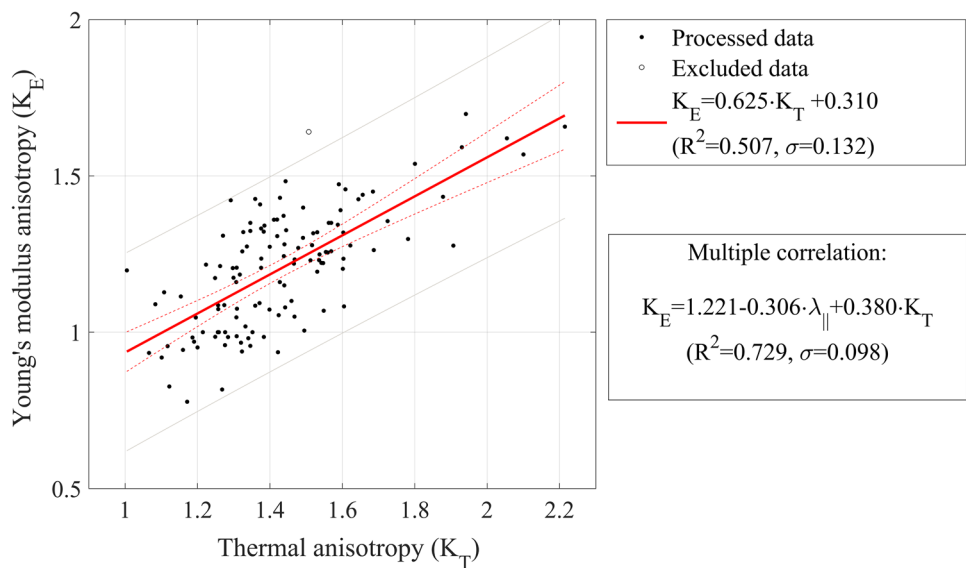

Well A   **Well B**   **Well C**

Fig. 7 Scatter plots of Young's modulus anisotropy $K_E = E_\parallel / E_\perp$ versus thermal anisotropy $K_T = \lambda_\parallel / \lambda_\perp$. The linear regression line (red) is shown with upper and lower 99% prediction bounds for a new observation (grey lines) or for the fitted curve (dashed lines in red). Taking into account the parallel component of thermal conductivity improves the fit, as seen from the multiple correlation box

- Processed data
- Excluded data
- $K_E = 0.625 \cdot K_T + 0.310$
  ($R^2 = 0.507$, $\sigma = 0.132$)

Multiple correlation:

$K_E = 1.221 - 0.306 \cdot \lambda_\parallel + 0.380 \cdot K_T$
($R^2 = 0.729$, $\sigma = 0.098$)

5 Discussion

Properties of shales, including anisotropy, are closely related to a partial alignment of anisotropic clay particles, kerogen inclusions, microcracks, low-aspect ratio pores and layering (Sayers 2013). Rock thermal property values of rocks vary significantly due to variations in mineralogical composition, porosity, fracturing, structure and texture, and the type and properties of pore-filling fluids. Typically, variations in thermal properties are informative at characterizing rock heterogeneity and are substantial within different formation scales, from macroscale to microscale (Popov et al. 2012). Analysis of

how thermal conductivity components vary with depth can help to predict variability in other material properties (e.g., strength, elastic moduli, and elemental composition). For example, if it is known that measured thermal heterogeneity is primarily driven by the heterogeneity of rock texture (e.g., the alignment of the clay constituents, their coordination number, and corresponding geometry of the pore space), it can be inferred that other rock properties, which are primarily affected by rock texture (e.g., electrical resistivity, permeability, elastic anisotropy) may exhibit a similar degree of heterogeneity (Popov et al. 2013). Rock properties in the Bazhenov formation are affected by both rock texture and composition (especially content of organic matter). We showed previously (Popov et al. 2015) that both thermal anisotropy and shear wave anisotropy are related to rock texture and are well correlated in formations with low-permeability. At the same time, strong contrast between thermal conductivity of the rock mineral matrix [2.3…3.0 W/(m·K) for formations with low-permeability] and thermal conductivity of kerogen [0.1…0.2 W/(m·K)] enables us to successfully predict the variation of total organic carbon with depth (Popov et al. 2016c). Bearing in mind these points and the close correlations established in the present work, thermal core logging should offer a high-resolution evaluation of elastic properties and anisotropy of the Bazhenov formation rocks.

5.1 Prediction of Elastic Wave Velocities and Density

The correlations, which have been established (see the formulas in Fig. 4), enable prediction and detailing of elastic velocities and density using the results of thermal conductivity profiling. The results, together with the logging data, are presented in Figs. 8 and 9, where every point on the plot represents average velocity (Fig. 8) or density (Fig. 9) determined for a core sample from its average thermal conductivity. Two different approaches were used to predict velocities: using only the parallel component of thermal conductivity (blue curve), and using only the perpendicular component (red curve).

There are rare intervals (e.g., the depth interval xx36–xx43 m in well B) where elastic wave velocities predicted via $\lambda_\perp$ are systematically less than elastic wave velocities predicted via $\lambda_\parallel$. We suggest that the systematic discrepancy in these depth intervals is explained by horizontal microcracks (not visible to the naked eye). Core samples are relaxed by microcracks generated during recovery to the surface (caused by unloading or drilling), and rock density in the respective intervals, measured in the laboratory, will then be systematically less than the logging density (Fig. 9). The thermal conductivity component $\lambda_\perp$ is reduced if horizontal microcracks appear, while $\lambda_\parallel$ is not changed, so velocity predicted via $\lambda_\perp$ becomes less than one predicted via $\lambda_\parallel$. This feature can be used to identify and select depth intervals, where samples exhibit horizontal microcracking after their recovery to the surface. Calculating $V_P(\lambda_\parallel)/V_P(\lambda_\perp)$ for each
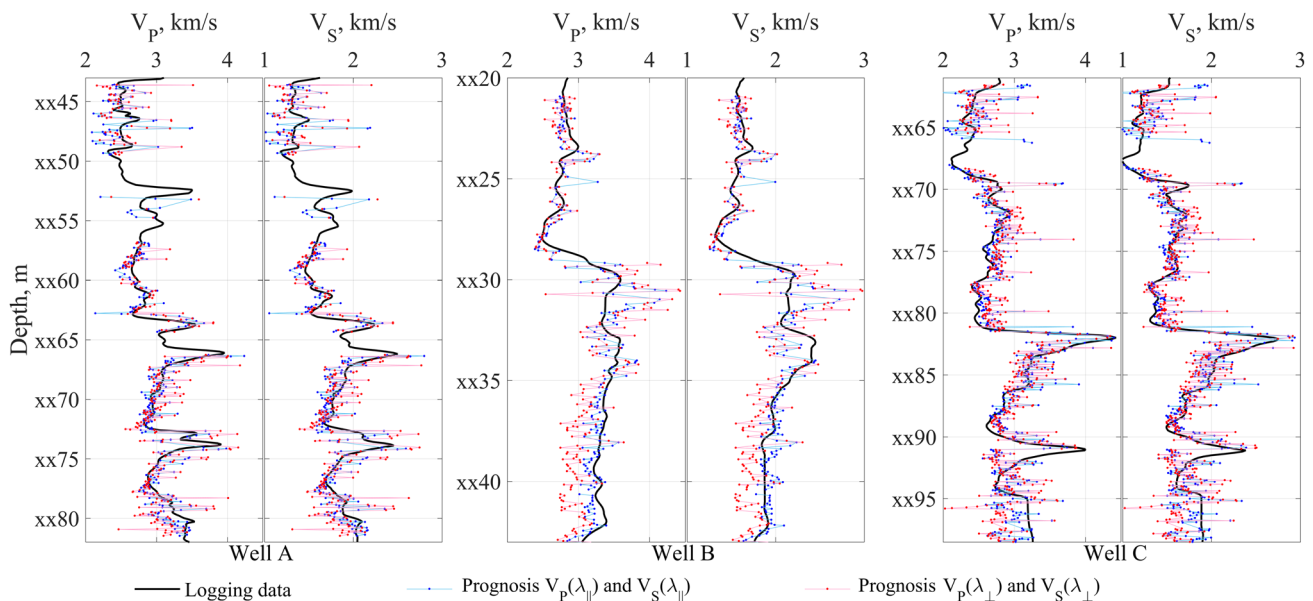

Fig. 8 Prediction and detailing of elastic wave velocities on the core scale using thermal conductivity profiles; comparison with logging data (black curve)
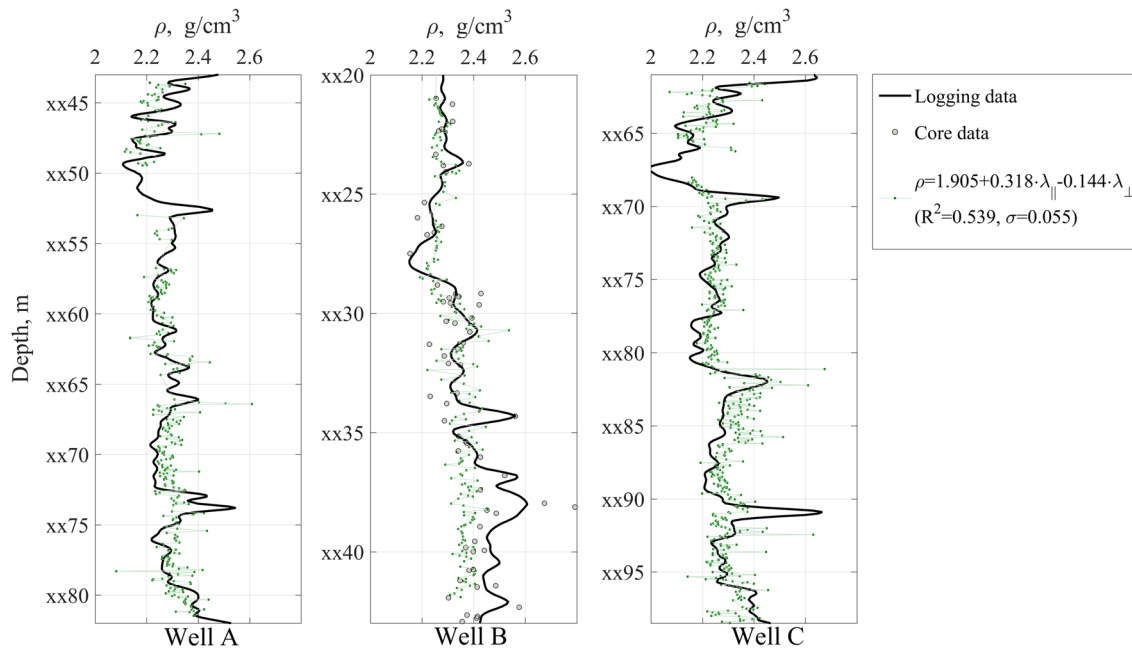
Fig. 9 Prediction and detailing of bulk density on the core scale using thermal conductivity profiles; comparison with logging data (black curve) and results of lab measurements on cores (black circles)

well (Fig. 10) we obtain the following empirical rule for the presence of such intervals:

$$\frac{\lambda_{||}}{0.82\lambda_{\perp} + 0.85} > 1. \tag{5}$$

It is interesting that the intervals were observed only in the lower part of the Bazhenov formation, which mainly contains silicites and is more brittle than the upper part of the formation.

The results shown justify the conclusion that, at least for the Bazhenov formation, continuous thermal profiling not only provides accurate and statistically representative evaluations of reservoir thermal properties, but can also contribute to effective determination (taking account of reservoir heterogeneity due to high spatial resolution) of depth intervals and the number of core samples needed for further geomechanical study in the laboratory. The fact that core logging can be carried out at core storages is a major advantage for practical purposes.

5.2 Prediction of Elastic Moduli

After predicting elastic velocities and density, the results of thermal conductivity profiling allow us to estimate the variation of dynamic Young's modulus E and Poisson's ratio ν with depth using the following formulas (Mavko et al. 1998):

$$E = \rho V_{S}^2 \frac{3V_{P}^2 - 4V_{S}^2}{V_{P}^2 - V_{S}^2}, \qquad \nu = 0.5 \frac{V_{P}^2 - 2V_{S}^2}{V_{P}^2 - V_{S}^2}. \tag{6}$$

The respective results on both the core scale and logging scale show a very good fit with logging data (Fig. 11). The few depth intervals where discrepancy is observed are mainly intervals that have vertical cracks of technogenic origin (e.g., the xx30–xx34 m depth interval in well B; the respective FMI image is shown in Fig. 6).

The lower part of the Bazhenov formation in the three studied wells has less kerogen volume fraction than the upper part, and this has impact on elastic moduli: on average, Young's modulus is lower in the upper part than in the lower part. This agrees with modelling results, showing that increase of kerogen inclusions lowers Young's moduli in shales (Sayers 2013). Poisson's ratio is greater in the upper part of the Bazhenov formation than in the lower part.

5.3 Prediction of Elastic Anisotropy Coefficients

The results of thermal core logging can also be used to estimate high-resolution Young's modulus anisotropy using established correlation (see the formula in the multiple correlation box in Fig. 7). The respective results fit very well with logging data (Fig. 12). In general, the Young's modulus parallel to bedding is greater than perpendicular to bedding, which is typical for shales (Sayers 2013).

As above, the few depth intervals with observed discrepancy are mainly intervals where there are vertical cracks of technogenic origin. The same situation is observed in Fig. 13, which shows prediction and detailing of the compressional and shear wave anisotropy coefficients via
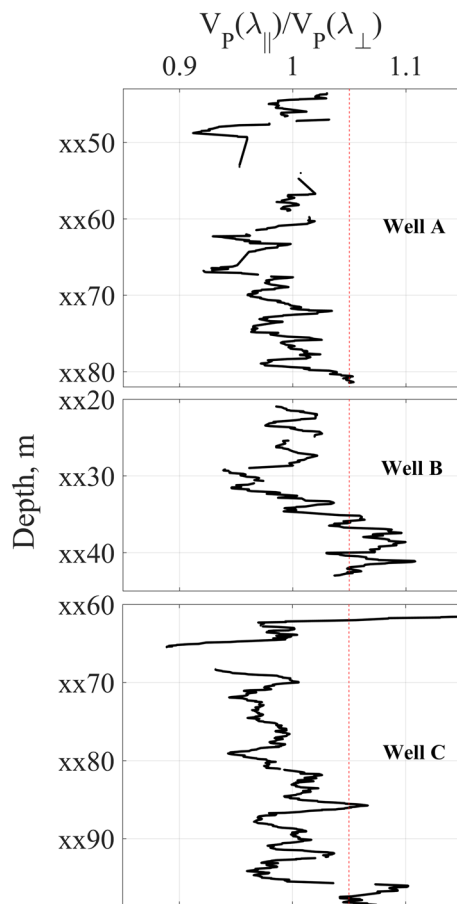
Fig. 10 Variation of the predicted compressional wave velocity ratio with depth for different wells (results are averaged in 50 cm moving windows). The ratio should be greater than 1.05 to select intervals where horizontal microcracks appear after core sample recovery to the surface

established correlations with thermal anisotropy coefficient (multiple correlation box in Fig. 5). The good fit with logging data makes us think that continuous thermal profiling in Bazhenov formations can be applied for rapid reservoir characterization in terms of Thomsen's γ and ε parameters (with vertical resolution, unachievable for well logging technique).

The results in Fig. 13 show decrease of anisotropy parameters with depth (from the top to the bottom of the Bazhenov formation), matching the trend of total organic carbon. This behavior agrees with published results of modelling, showing that the presence of kerogen inclusions lowers Thomsen anisotropy parameters (Sayers 2013).

6 Conclusions

The novel approach based on thermal core logging was tested on 1062 full-diameter core samples (with total length more than 100 m) from three wells drilled through the Bazhenov formation at an oilfield in the West Siberian Basin. The approach provided high-resolution evaluation of elastic properties and anisotropy of unconventional reservoir rocks. The strong correlations of principal components of thermal conductivity tensor with elastic velocities and rock density as well as correlations of thermal anisotropy coefficient with Young's modulus anisotropy and Thomsen's parameters that were established can help to better explain the behavior of thermal and elastic rock properties of the Bazhenov formation, predict one property from another and enrich the database of organic-rich shales. Successful comparison of elastic properties predicted from the thermal core logging data with well logging data as well as the results of previous investigations lead us to believe that the technique is viable for unconventional formations.

Found correlations are primarily driven by the presence of organic matter in formation and the contrast between properties (e.g., thermal conductivity, density, elastic wave velocities) of the rock mineral matrix and kerogen; for thermal conductivity the contrast is very strong, higher than 10:1. The correlations can be used for low-permeable, organic-rich unconventional formations with the similar sedimentation features. Another kerogen type or maturity level may affect the found correlations. Universality of found correlations for entire depth interval is coming from small variations of the rock mineral matrix properties along depth within the Bazhenov formation of the given oilfield. Universal correlation for entire depth interval cannot be constructed if there are two or more lithologies with different rock matrix properties in the formation (like in the Domanik formation); in such cases, several correlations will be observed.

The thermal core logging equipment is easy to transport (the measurements can be carried out at core storages) and has non-contact, non-destructive, high-resolution features. It can, therefore, be used to help obtain rapid characterization of a reservoir in terms of thermal and elastic properties, including effective determination of depth intervals and the number of cores needed for further geomechanical study of the rocks (particularly heterogeneous rocks) in the laboratory.
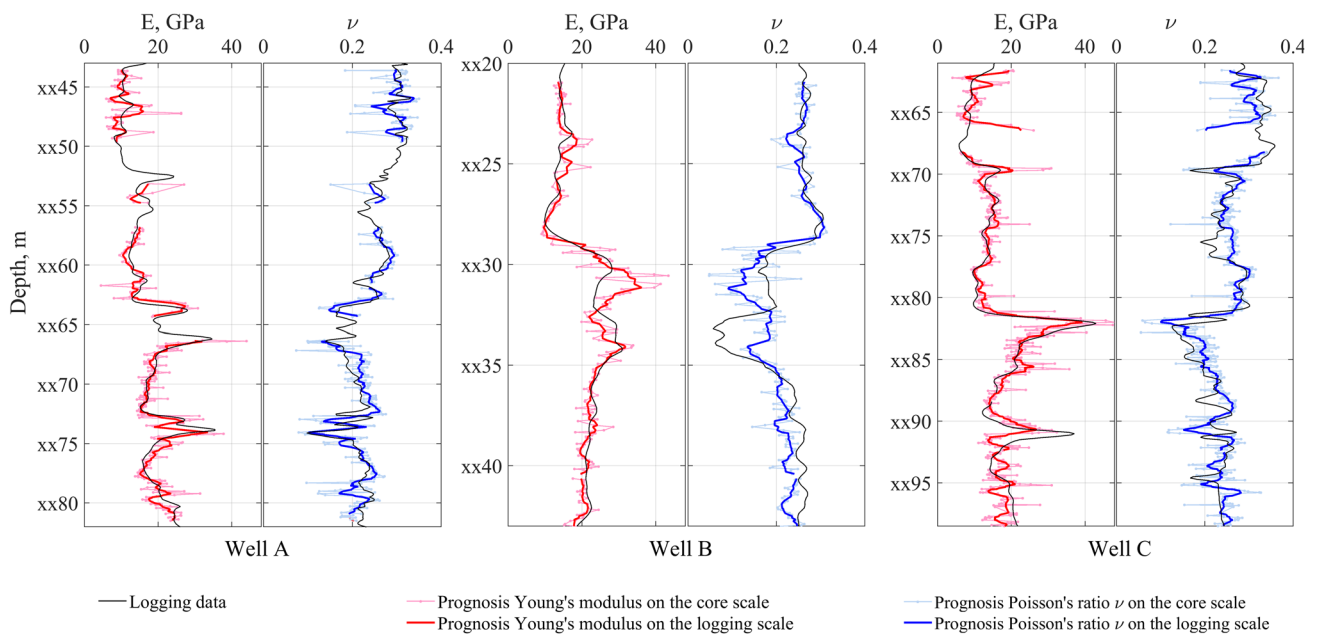
Fig. 11 Prediction and detailing of elastic moduli (colored curves) using results of thermal profiling in comparison with logging data (black curves)
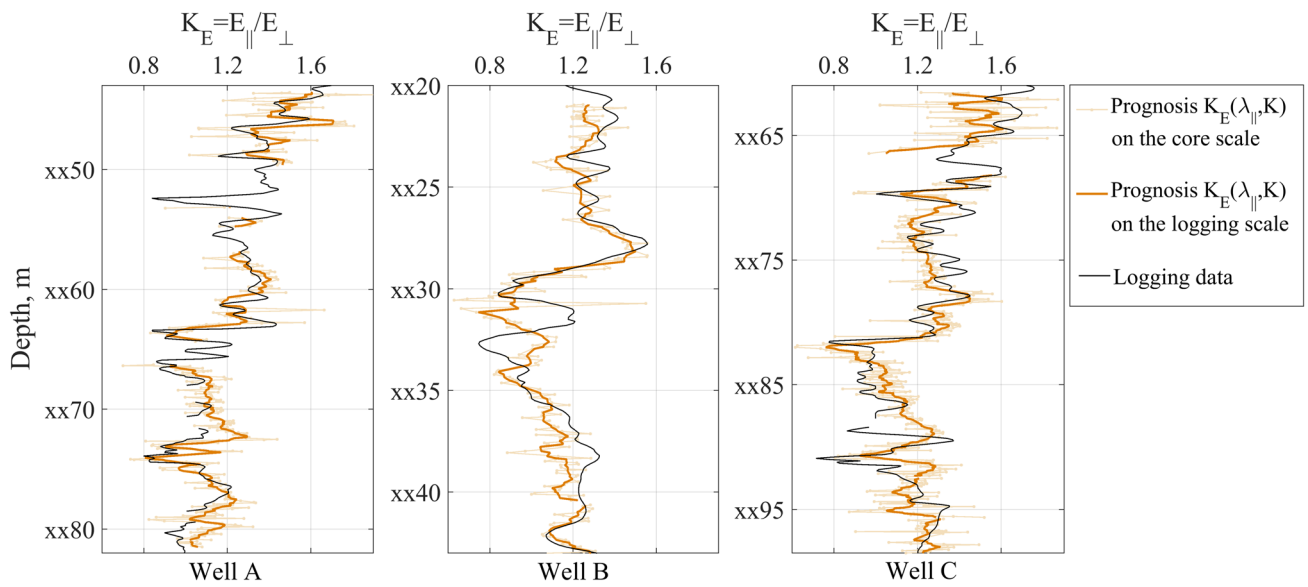

Fig. 12 Prediction and detailing of Young's modulus anisotropy (colored curves) using results of thermal profiling and established correlations; comparison with logging data (black curves)
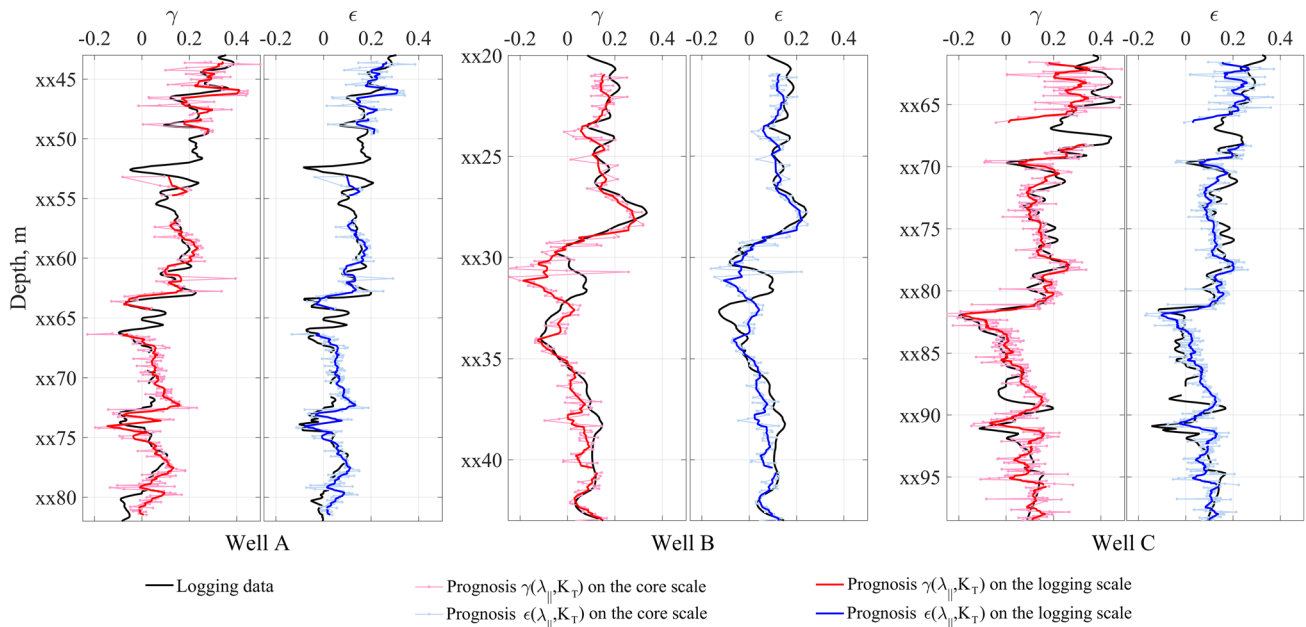
Fig. 13 Prediction and detailing of Thomsen's parameters (colored curves) using the results of thermal profiling and established correlations (multiple correlation box in Fig. 5); comparison with logging data (black curves)

References

Alford RM (1986) Shear data in the presence of azimuthal anisotropy: Dilley, Texas. In: SEG technical program expanded abstracts, pp 476–479. https://doi.org/10.1190/1.1893036

Armstrong P, Ireson D, Chmela B, Dodds K, Esmersoy C, Miller D, Hornby B, Sayers C, Schoenberg M, Leaney S, Lynn H (1994) The promise of elastic anisotropy. Oilfield Rev 6:36–47

Brie A, Codazzi D, Esmersoy C, Hsu K, Denoo S, Mueller MC, Plona T, Shenoy R, Sinha B (1998) New directions in sonic logging. Oilfield Rev 10(1):40–55

Brown J, Davis B, Gawankar K, Kumar A, Li B, Miller CK, Laronga R, Schlicht P (2015) Imaging: getting the picture downhole. Oilfield Rev 27(2):4–21

Chekhonin E, Parshin A, Pissarenko D, Popov Y, Romushkevich R, Safonov S, Spasennykh M, Chertenkov M, Stenin V (2012) When rocks get hot: thermal properties of reservoir rocks. Oilfield Rev 24(3):20–37

Chekhonin E, Popov E, Popov Y, Spasennykh M, Zhukov V, Ovcharenko Y, Karpov I, Zagranovskaya D (2016) Geomechanical data quality improvement for Bazhenov formation rocks via thermal core logging. In: Proceedings of 18th conference "Geomodel 2016". Russia, Gelendzhik, 12–15 Sep (in Russian). https://doi.org/10.3997/2214-4609.201602280

Franco JLA, De GS, Renlie L, Williams S (2006) Sonic investigations in and around the borehole. Oilfield Rev 18(1):14–33

Goligher A, Scanlan B, Standen E, Wylie AS (1996) A first look at platform express measurements. Oilfield Rev 8(2):5–15

Keir D, McIntyre B, Hibbert T, Dixon R, Koster K, Mohamed F, Donald A, Syed A, Liu C, O'Rourke T, Paxton A, Horne S, Knight ED, Sayers S, Primiero P (2011) Correcting sonic logs for shale anisotropy: a case study in the Forties field. First Break 29:81–86

Kim H, Cho JW, Song I, Min KB (2012) Anisotropy of elastic moduli, P-wave velocities, and thermal conductivities of Asan Gneiss, Boryeong Shale, and Yeoncheon Schist in Korea. Eng Geol 147:68–77

Mavko G, Mukerji T, Dvorkin J (1998) The rock physics handbook, 1st edn. Cambridge University Press, Cambridge

Özkahraman HT, Selver R, Isik EC (2004) Determination of the thermal conductivity of rock from P-wave velocity. Int J Rock Mech Min Sci 41:703–708

Pimienta L, Sarout J, Esteban L, Piane CD (2014) Prediction of rocks thermal conductivity from elastic wave velocities, mineralogy and microstructure. Geophys J Int 197(2):860–874

Pistre V, Sinha BK (2008) Applications of sonic waves in the estimation of petrophysical, geophysical and geomechanical properties of subsurface rocks. In: IEEE ultrasonics symposium proceedings: pp 78–85. https://doi.org/10.1109/ULTSYM.2008.0020

Popov Y (1997) Optical scanning technology for non-destructive contactless measurements of thermal conductivity and diffusivity of solid matter. In: Giot M, Mayinger F, Celata GP (eds) Experimental heat transfer, fluid mechanics and thermodynamics. Proceedings of the 4th world congress on experimental heat transfer, fluid mechanics and thermodynamics, vol 1, Belgium, Brussels, pp 109–116

Popov Y, Mandel A (1998) Geothermal study of anisotropic rock masses. Izv Phys Solid Earth 34(11):903–915

Popov Y, Berezin V, Soloviov G, Romuschkevitch R, Korostelev V, Kostiurin A, Kulikov A (1987) Thermal conductivity of minerals. Izv Phys Solid Earth 23(3):245–253

Popov Y, Tertychnyi Y, Romushkevich R, Korobkov D, Pohl J (2003) Interrelations between thermal conductivity and other physical properties of rocks: experimental data. Pure Appl Geophys 160:1137–1161

Popov Y, Parshin A, Chekhonin E, Gorobtsov D, Miklashevskiy D, Korobkov D, Suarez-Rivera R, Green S (2012) Rock heterogeneity from thermal profiles using an optical scanning technique. In: Proceedings of 46th US rock mechanics/geomechanics symposium. Chicago, IL, USA, 24–27 June. ARMA 12–509

Popov Y, Parshin A, Chekhonin E, Popov E, Miklashevskiy D, Suarez-Rivera R, Green S (2013) Continuous core thermal properties measurements and analysis. In: Proceedings of 47th US rock mechanics/geomechanics symposium. San Francisco, CA, USA, 23–26 June. ARMA 13–391, 4: 2991–2999

Popov Y, Mikhaltseva I, Chekhonin E, Popov E, Romushkevich R, Kalmykov G, Latypov I (2015) Improving quality of rock anisotropy study by combining sonic logging and thermal conductivity measurements on cores. In: Proceedings of 17th conference "Geomodel-2015". Russia, Gelendzhik, 7–10 Sep (in Russian). https://doi.org/10.3997/2214-4609.201413949

Popov Y, Popov E, Chekhonin E (2016a) New facilities in rock thermal property measurements in application to geomechanics. In: Ulusay R, Aydan O, Gercek H, Hindistan MA, Tuncay E (eds) Rock mechanics and rock engineering: from the past to the future. Taylor & Francis Group, London, pp 199–204. https://doi.org/10.1201/9781315388502-33

Popov Y, Beardsmore G, Clauser C, Roy S (2016b) ISRM suggested methods for determining thermal properties of rocks from laboratory tests at atmospheric pressure. Rock Mech Rock Eng 49:4179–4207. https://doi.org/10.1007/s00603-016-1070-5

Popov E, Chekhonin E, Popov Y, Romushkevich R, Gabova A, Zhukov V (2016c) Novel approach to Bazhenov formation study through core thermal profiling. Nedropolzovanie XXI vek 6(63):52–61 **(in Russian)**

Sayers CM (2013) The effect of anisotropy on the Young's moduli and Poisson's ratios of shales. Geophys Prospect 61:416–426. https://doi.org/10.1111/j.1365-2478.2012.01130.x

Schoenberg M, Muir F, Sayers C (1996) Introducing ANNIE: a simple three-parameter anisotropic velocity model for shales. J Seism Explor 5:35–49

Scott DW (1979) On optimal and data-based histograms. Biometrika 66(3):605–610. https://doi.org/10.1093/biomet/66.3.605

Suarez-Rivera R, Bratton T (2009) Estimating horizontal stress from three-dimensional anisotropy: US Patent 20090210160

Thomsen L (1986) Weak elastic anisotropy. Geophysics 51(10):1954–1966

Togashi Y, Kikumoto M, Tani K (2017) An experimental method to determine the elastic properties of transversely isotropic rocks by a single triaxial test. Rock Mech Rock Eng 50:1–15. https://doi.org/10.1007/s00603-016-1095-9

Tsvankin I (2012) Seismic signatures and analysis of reflection data in anisotropic media. Society of exploration geophysicists. Third edn. https://doi.org/10.1190/1.9781560803003

Ulmishek GF (2003) Petroleum Geology and Resources of the West Siberian Basin, Russia. US Geological Survey Bulletin 2201-G. US Geological Survey, Reston, Virginia. https://pubs.usgs.gov/bul/2201/G/. Accessed 6 Sept 2017